1521-009X/42/2/274–281$25.00
Drug Metabolism and Disposition
http://dx.doi.org/10.1124/dmd.113.053694
Drug Metab Dispos 42:274–281, February 2014

Metabolism of Salvianolic Acid A and Antioxidant Activities of Its Methylated Metabolites

Hui Xu, Yanli Li, Xin Che, Hongcui Tian, Huaying Fan, and Ke Liu

School of Pharmacy, Yantai University, Yantai, China

Received July 12, 2013; accepted November 25, 2013

ABSTRACT

This study investigated the metabolism of salvianolic acid A (SAA) both in vivo and in vitro. Liquid chromatography–mass spectrometry analysis of drug-containing rat bile samples and bile samples hydrolyzed by glucuronidase revealed a series of methylated conjugates of SAA and its glucuronides, as well as the predominance of the methylation pathway of SAA in rats. For the first time, four major methylated metabolites present in vivo were prepared for structure characterization and bioactivity evaluation using in vitro coincubation systems with rat hepatic cytosol protein as the enzyme donor. By using nuclear magnetic resonance imaging and other spectroscopic methods, these metabolites were unambiguously elucidated as 3-*O*-methyl-SAA (M1), 3′-*O*-methyl-SAA (M2), 3,3″-*O*-dimethyl-SAA (M3), and 3′,3″-*O*-dimethyl-SAA (M4), respectively. Along with results from the enzyme inhibition study, selective formation of these *meta*-*O*-methylated derivatives indicated that catechol *O*-methyltransferase (COMT) is responsible for methylated transformation of SAA. All of these metabolites displayed fairly high antioxidant potency against in vitro rat liver lipid peroxidation with half-maximal inhibitory concentrations that were much lower than those of the positive controls and even SAA. Overall, the results from this study demonstrate that SAA is a metabolically unstable compound that undergoes rapid methylation metabolism catalyzed by COMT, and these generated *O*-methylated metabolites may be largely responsible for its in vivo pharmacological effects.

Introduction

Danshen is a type of well known traditional Chinese herbal medicine prepared from the dried roots and rhizomes of *Salvia miltiorrhiza* Bge. (Labiatae). With its ability to enter the channel of heart, pericardium, and liver, Danshen is able to promote blood circulation and remove stasis and is extensively used clinically to treat and prevent many diseases, including hepatitis, hepatocirrhosis, chronic renal failure, dysmenorrhea, neurasthenic insomnia, and ischemic injuries (Wasser et al., 1998; Ji et al., 2000; Zhou et al., 2005; Cheng, 2006). During the past 2 decades, research interest in the water-soluble components of Danshen was initially motivated by its uses in water decoction in traditional Chinese prescriptions and in injection treatments for cerebral and coronary vascular diseases (Wang et al., 2007). Caffeic acid derivatives are the major water-soluble components of Danshen. More than 20 salvianolic acids (SAs), the caffeic acid oligomers, have been isolated from Danshen to date (Lu and Foo, 2002; Ho and Hong, 2011).

Salvianolic acid A (SAA) is a type of caffeic acid trimer biosynthesized from condensation of caffeic acid and Danshensu at a molar ratio of 2:1 (Fig. 1) (Li et al., 1984). In recent years, SAA has drawn great research attention for its diverse potent bioactivities, including antioxidative, antiplatelet, and antithrombotic effects (Huang and Zhang, 1992; Wang et al., 2005; Fan et al., 2010). Among various SAs, SAA has been found to display the most potent protective action against peroxidative damage to biomembranes (Liu et al., 1992). Considerable evidence has also demonstrated the potent protective effects of SAA against ischemia-induced injury both in vitro and in vivo (Wang et al., 2009; Pan et al., 2011; Fan et al., 2012).

It is well known that phenolic acids (including SAs) are likely to undergo phase II conjugation metabolism, and the biliary route of elimination is considered to be most import to the in vivo disposition of these compounds (Baba et al., 2004; Zhang et al., 2004; Lv et al., 2010). Pharmacokinetic studies indicate that SAA has extremely low bioavailability and very short plasma elimination half-time (Hou et al., 2007; Pei et al., 2008). Our previous study of rats after intravenous administration of SAA (unpublished data) also revealed that there were various metabolites found in bile, and SAA excreted as an unchanged form was very limited (0.57% and 2.74% into urine and bile, respectively). All of these findings suggest that metabolism is an important elimination pathway of SAA, and pharmacological activities in vivo may be related to its metabolic fate. Five conjugated metabolites of SAA (including methylated, glucuronidated, and both) were identified from rat plasma, indicating methylation and glucuronidation as the two main in vivo metabolic pathways of SAA in rats (Shen et al., 2009). The kinetics of SAA glucuronidation by pooled human microsomes and recombinant UDP-glucuronosyl transferase (UGT) isozymes were recently studied, and UGT1A1 and UGT1A9 were identified as the major human UGT isoforms that catalyze the glucuronidation of SAA (Han et al., 2012). However, the methylation characteristics of SAA have not been systematically evaluated, which is the objective of this study.

This research was supported by the National Natural Science Foundation of China [Grant 81102780] and the Natural Science Foundation of Shandong Province [Grant ZR2013HZ004].

dx.doi.org/10.1124/dmd.113.053694.

ABBREVIATIONS: BHT, 2,6-di(tert-butyl)-4-hydroxytoluene; COMT, catechol *O*-methyltransferase; ESI, electrospray ionization; HPLC, high-performance liquid chromatography; LC-MS, liquid chromatography–mass spectrometry; RHC, rat hepatic cytosol; SA, salvianolic acid; SAA, salvianolic acid A; SAB, salvianolic acid B; SAM, *S*-adenosyl-L-methionine; TBA, thiobarbituric acid; TIC, total ion current; UGT, UDP-glucuronosyl transferase; XIC, extracted ion current.

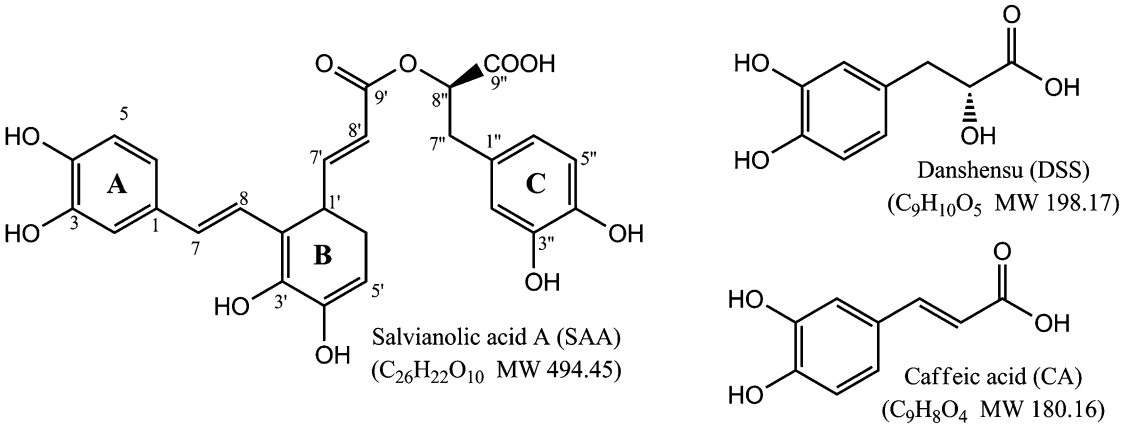

Fig. 1. Chemical structure of SAA.

To analyze in vivo metabolite profiles in rats and in in vitro enzyme-catalyzed methylation, the enzymes responsible for methylation of SAA were confirmed and four major methylated metabolites of SAA present in vivo were prepared using an in vitro incubation system. For the first time, the chemical structures of these methylated metabolites were unambiguously identified by spectroscopic methods, and their antioxidant activities were evaluated. The findings from the present study have provided convincing evidence to understand the metabolism mechanism of SAA and bioactivities of its metabolites.

Materials and Methods

Chemicals and Other Reagents. SAA with 99.5% purity was provided by Shandong Target Drug Co. Ltd (Yantai, China). *S*-adenosyl-L-methionine (SAM), entacapone, trichloroacetic acid, thiobarbituric acid (TBA), and β-glucuronidase from *Escherichia coli* were purchased from Sigma Chemical Co. (St. Louis, MO). 2,6-di(tert-butyl)-4-hydroxytoluene (BHT) and α-tocopherol (95%) were obtained from Sinopharm Chemical Reagent Co. Ltd. (Beijing, China) and FlukaChemieAG (Buchs, Switzerland), respectively. All of the remaining chemicals and solvents used were of standard analytical or high-performance liquid chromatography (HPLC) grade. Ultrapure water prepared by a Milli-Q system (Millipore, Bedford, MA) was used throughout the study.

Animals. Male Sprague-Dawley rats weighing 180–220 g were obtained from the Laboratory Animal Center of Shandong Luye Pharmaceutical Co. Ltd (Yantai, China). They were provided with standard laboratory food and water and maintained on a 12-hour light/dark cycle in an air-conditioned animal quarter at constant temperature (22–24°C) and humidity (50% ± 10%). The animals were fasted overnight with free access to water before any experiment. The animal experiments were conducted in accordance with the local institutional guidelines for care and use of laboratory animals at Yantai University.

In Vivo Metabolism in Rats. Eight rats were evenly divided into two groups at random. The animals were fixed on a wooden plate and anesthetized with diethyl ether. An abdominal incision was made and the common bile duct was cannulated with PE-10 tubing (0.8 mm i.d.; Becton Dickinson, Franklin Lakes, NJ) for bile collection. After recovery from anesthesia, one group received a single 20 mg/kg intravenous dose of SAA in saline and the drug-containing bile samples were collected into successive vials on ice at different time points over a 12-hour period. The blank samples were collected from the other group after intravenous dosing of the same volume of saline. Hydrolysis of drug-containing bile samples with β-glucuronidase was performed according to the method of Han et al. (2012). For subsequent analysis, all of the bile samples were first subjected to liquid–liquid extraction as follows. An aliquot of a 2-ml bile sample was extracted with 3 volumes of ethyl acetate after the addition of 300 μl hydrochloric acid (1 M). The supernatant was separated after vortex-mixing for 5 minutes and centrifugation at 8000*g* for another 5 minutes, and then evaporated to dryness under a stream of nitrogen at 35°C. The residue was reconstituted into 300 μl mobile phase by vortex-mixing for 1 minute and then centrifuged at 15,000*g* for 10 minutes to obtain the supernatant for analysis.

In Vitro Methylation. Immediately after euthanasia, the rat livers were removed and homogenized with 9 volumes of 1.15% KCl, and then centrifuged at 12,000*g* for 15 minutes at 4°C. The supernatant (S9 fraction) was further centrifuged at 100,000*g* for 90 minutes to obtain microsomal and cytosol fractions. The incubation systems contained 6.8 mg rat hepatic cytosolic (RHC) protein, 5 mM $MgCl_2$, and 1 mM SAM as the exogenous methyl donor in 50 mM phosphate buffer solution (pH 7.4). When confirming the enzyme responsible for methylation, entacapone, a selective catechol *O*-methyl transferase (COMT) inhibitor, was added at a concentration of 3 μM. After preincubation at 37°C for 5 minutes, SAA was added into the mixture at a final concentration of 0.25 mM and subjected to further incubation for 15 minutes at 37°C. The reaction was then terminated by adding 5 M HCl, and the mixture was extracted with 3 volumes of ethyl acetate. After vortex-mixing for 5 minutes and centrifugation at 8000*g* for 10 minutes, the supernatant was separated and evaporated to dryness for subsequent HPLC assay and preparative separation.

Separation of Methylated Metabolites by Column Chromatography. The terminated incubation samples from several batches were combined, diluted with water, and applied to a Strata-X solid phase extraction column (Phenomenex, Torrance, CA). After washing with both water and MeOH/H_2O (20:80) for 8 column volumes, the column was then eluted with 10 column volumes of MeOH/H_2O (55:45) to obtain eluent for further repeated column chromatography using C18 (10 mm × 200 mm i.d., YMC-pack ODS-A, 5 μm), which was gradient eluted with the mixture of MeOH and 0.05% formic acid. According to the elution order, four compounds named M1 (15 mg), M2 (12 mg), M3 (8 mg), and M4 (5 mg) were obtained.

Chemical Structure Characterization. Ultraviolet (UV) and infrared (IR) spectra were measured on a Shimadzu UV-2550 (Shimadzu, Kyoto, Japan) and Nicolet 6700 FT-IR spectrometer (Thermo Nicolet Corp., Madison, WI), respectively. Electrospray ionization mass spectroscopy (ESI-MS) data were determined in negative ion mode using a triple quadrupole mass spectrometer from Thermo Fisher Scientific Inc. (Waltham, MA). One-dimensional and two-dimensional nuclear magnetic resonance (NMR) spectra were recorded on a Bruker AV400 NMR spectrometer (Bruker Co., Faellanden, Switzerland) operating at 400 MHz for protons and 100 MHz for carbon in methanol-*d*4 at room temperature. Chemical shifts were expressed as values (parts per million) relative to the internal standard, tetramethylsilane.

Analytical HPLC Conditions. The chromatographic system used for detecting metabolites was an Agilent 1100 HPLC (Agilent Technologies, Santa Clara, CA) equipped with a binary pump, autosampler, column manager, and variable wavelength detector. HPLC analysis was performed on an Xterra RP18 column (150 mm × 4.6 mm i.d., 3.5 μm; Waters Corporation, Milford, MA) and the column temperature was maintained at 30°C. The mobile phase composed of a mixture of acetonitrile (A) and 0.05% formic acid (B) was delivered at a flow rate of 1 ml/min. For in vivo metabolism studies, a linear gradient elution was performed to run the separation, and the elution program was conducted as follows: 0–29 minutes, holding at 25% A; 29–31 minutes, a linear increase from 25% A to 30% A; 31–60 minutes, holding at 30% A; 60–62 minutes, a linear decrease from 30% A to 25% A; and 62–75 minutes, holding at 25% A. An isocratic elution mode with 30% A and 70% B was used for in vitro

incubation systems. The injection volume was set at 20 μl, and HPLC detection was conducted at 285 nm according to the maximum absorption of SAA.

LC-MS Qualitative Analysis. A TSQ Quantum Access triple quadrupole tandem mass spectrometer (Thermo Fisher Scientific Inc.) was connected to the HPLC system via an ESI interface. Ultrahigh-purity helium was used as the damping and collision gas, and nitrogen was used as the sheath and auxiliary gas. The ESI source was operated in negative ion mode from *m/z* 150 to 900. Other MS conditions for maximum detection of metabolites were set as follows: spray voltage, 3.5 kV; capillary temperature, 350°C; capillary voltage, −30 V; sheath gas, 30 psi and 0.75 l/min; auxiliary gas, 5 psi and 0.15 l/min; and collision gas, 1.5 mTorr and 0.75 l/min. The HPLC conditions were set as described above. Both system control and data processing were performed using Xcalibur (Thermo Fisher Scientific Inc.) workstation software (version 1.4.1).

Assay of Lipid Peroxide in Rat Liver Homogenate. This assay is based on the reaction of malondialdehyde with TBA forming an malondialdehyde-TBA2 adduct and was performed as described by Chai et al. (2012) with slight modification. Male Sprague-Dawley rats with a body weight of 220 ± 20 g were euthanized and livers were isolated after disposing of blood. The livers were then cut into slices and homogenated with saline to obtain 2% tissue homogenate for use. An aliquot of 0.25 ml liver homogenate was mixed with 1.0 ml test sample solution (dissolved with phosphate-buffered saline at different concentrations), 50 μl ferrous ammonium sulfate solution (1 mM), and 50 μl vitamin C solution (1 mM) to initiate the reaction. The mixtures were incubated at 37°C for 1 hour, and then 1.0 ml trichloroacetic acid solution (20%) was added to stop the oxidation reaction. After mixing and standing for 10 minutes, the reaction solution was centrifuged at 3000 *g* for 10 minutes. The supernatant was added with 0.25 ml TBA solution (3.2%) and delivered to a boiling water bath for 20 minutes. After cooling down, the absorption of the solution was determined at 532 nm. The inhibitory rate on lipid peroxidation was calculated by referring to the blank control. All of the experiments were performed in triplicate, and data are expressed as the mean ± S.D. of three independent experiments. Statistical analysis of the data were performed using one-way analysis of variance. Differences with $P < 0.05$ were considered statistically significant.

Results

In Vivo Metabolism of SAA in Rats. Rat urine was collected and quickly analyzed. However, excretion of SAA conjugative metabolites was minimal in this matrix and thus the analysis focused on bile. Taking into account the composition complexity of the drug-containing bile sample, an LC-MS assay based on gradient chromatographic elution mode was developed to fully display the biliary metabolite profile as much as possible. A linear gradient elution of eluents A (acetonitrile) and B (0.05% formic acid) was well optimized and performed to run the separation within an overall runtime of 70 minutes. For more exact qualitative characterization, the extracted ion current (XIC) chromatograms created via a special data-mining process were recovered from the entire data set for a chromatographic run, the total ion current (TIC) chromatogram. In view of the two main in vivo metabolic pathways of SAA in rats, methylation and glucuronidation (Shen et al., 2009), the extracted *m/z* values of $[M\text{-}H]^-$ ions representing SAA and all of its conjugative metabolites of interest included the following: 493 (SAA); 507, 521, and 535 (monomethyl SAA, dimethyl SAA, and trimethyl SAA); and 669, 683, 697, and 711 (glucuronides of SAA, and monomethyl, dimethyl, and trimethylmethyl SAA, respectively). The HPLC-UV, TIC and XIC chromatograms of the drug-containing bile and blank bile samples are shown in Fig. 2 and detailed LC-MS data are listed in Table 1.

Based on LC-MS profiling of bile, more than 20 metabolites with peak intensity larger than 3.5×10^4 were detected, including SAA, 10 methylation products of SAA (3 monomethyl, 5 dimethyl, and 2 trimethyl), 1 glucuronide of SAA, as well as 13 underlying methylated metabolites showing both methylation and glucuronidation (as shown in Table 1). The XIC filtered chromatograms (Fig. 2F) clearly demonstrated that both the two largest metabolite peaks in bile (marked as L1 and L2 in Fig. 2D) were dimethyl glucuronide of SAA, with an *m/z* value of 697. Compared with the reference standards obtained from in vitro preparation as discussed below, the other four major methylation products with retention times of 29.69 minutes, 34.58 minutes, 41.57 minutes, and 44.87 minutes were chromatographically identified as 3-*O*-methyl-SAA (M1), 3′-*O*-methyl-SAA (M2), 3,3′′-*O*-dimethyl-SAA (M3), and 3′,3′′-*O*-dimethyl-SAA (M4), respectively. Many methylated and underlying methylated conjugates of SAA abundant in drug-containing bile provide convincing evidence for the predominance of its in vivo methylation pathway in rat. These findings also reveal that in rats, SAA is prone to undergoing rapid hepatic metabolism and high biliary excretion in the form of methylated conjugates, which is similar to the metabolic characteristics observed in some other natural phenolic acids, including salvianolic acid B (SAB), caffeic acid, and rosmarinic acid (Baba et al., 2004; Xu et al., 2007; Lv et al., 2010).

To examine the relative distribution of all of these methylation conjugates of SAA, a hydrolysis study was further conducted on the drug-containing rat bile sample using β-glucuronidase to cleave all of the glucuronides of SAA back to their aglycones. LC-MS analysis was performed for the hydrolyzed bile under the same conditions as the untreated sample, which clearly revealed the full set of methylation products in the absence of all of the glucuronides, as well as the difference in methylation product profiling between these two bile samples. As shown in Fig. 3 and Table 1, after hydrolysis by β-glucuronidase, the relative distribution of monomethyl SAA at 30.68 min to the whole monomethylation products significantly increased from approximately 3% to 16%. An increase from 23% to 30% in the relative distribution of dimethyl SAA at 44.87 min to the whole dimethylation products was also observed. According to the retention time and *meta*-*O*-methylation of SAA catalyzed by COMT, these two metabolites could be deduced as 3′′-*O*-monomethyl-salvianolic acid A, and 3′, 3′′-*O*-dimethyl-SAA (M4), respectively. All of these findings suggest that 3′′-*O*-methyl-SAA is much more reactive than M1 or M2, and is very easily subjected to conjugative reaction (including methylation and glucuronidation). Eventually this methylation product is rapidly transformed into more stable subsequent conjugative metabolites of SAA such as M3, M4, and 3′′-*O*-methyl-salvianolic acid A glucuronide. This may be why there is a very limited amount of this 3′′ monomethyl metabolite but fairly high levels of M1 to M4 found in rat bile.

In Vitro Methylation in a RHC Incubation System. Based on the above in vivo findings that SAA could be rapidly metabolized into a series of methylated conjugates by rat hepatic enzymes, in vitro enzyme-catalyzed incubation using a rat hepatic subcellular fraction as the enzyme donor was performed to elucidate the mechanism of in vivo methylation and prepare major methylated metabolites of SAA for further studies on structure and activity. The COMT activities of rat liver subcellular fractions were determined as 0.753±0.106, 0.742±0.100, and 0.146±0.032 $pmol \cdot mg^{-1} \cdot min^{-1}$ ($n = 6$) for S9, cytosol, and microsomes, respectively. The hepatic cytosol displayed much higher COMT activity than microsomes ($P < 0.05$) and contained much less endogenous interfering substances than the S9 fraction. Therefore, the in vitro enzyme-catalyzed biotransformation of SAA was carried out in the incubation system using RHC as the enzyme donor. The optimal incubation conditions were established according to our previous study on the enzyme kinetics of this incubation system.

Several different incubation systems were constructed as controls, including the blank control without SAA, the negative control containing SAA, SAM, and heat-inactivated RHC, and the control containing entacapone, a selective COMT inhibitor. First, a feasible

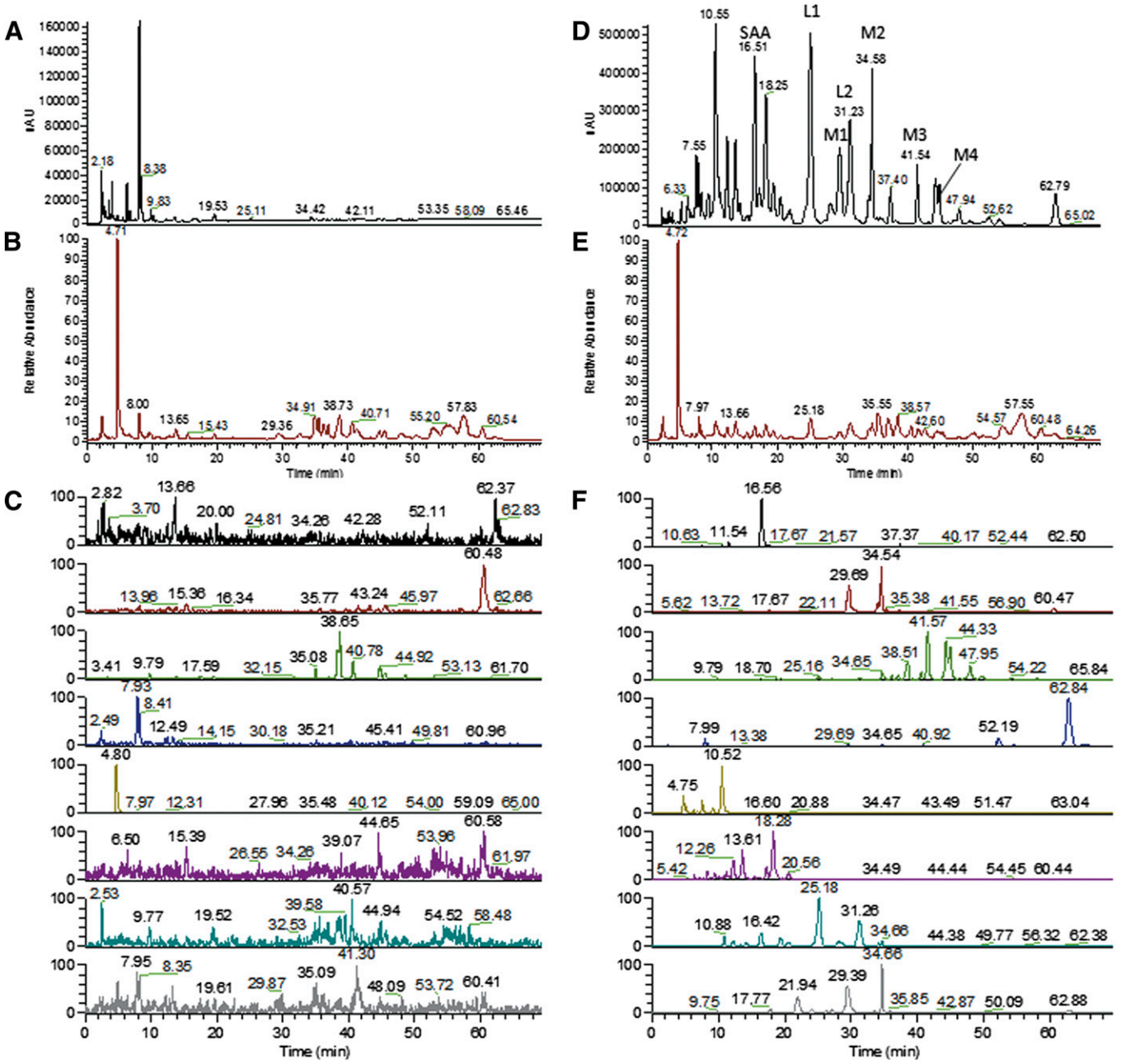

Fig. 2. HPLC-UV, TIC and XIC chromatograms of the drug-containing rat bile and the blank control. HPLC-UV (A), TIC (B), and XIC (C) chromatograms of the blank bile, and HPLC-UV (D), TIC (E), and XIC (F) chromatograms of the drug-containing rat bile sample, respectively. SAA, M1, M2, M3, M4, L1, and L2 labeled in (D) indicated the parent compound, the four isolated methylation products, and the two largest peaks present in rat bile, respectively. (C and F) The extracted *m/z* values in the XIC chromatograms were 493, 507, 521, 535, 669, 683, 697, and 711 from top to bottom.

HPLC method differing from that for the study of in vivo metabolism was developed for fast and effective separation of methylation products using an isocratic elution of acetonitrile and 0.05% formic acid (30:70, *v/v*) within an overall runtime of 30 minutes. To verify the consistency between in vitro and in vivo metabolism, the drug-containing rat bile sample was used a reference and subjected to further HPLC detection under the conditions for these in vitro incubation systems. The discrepancy between Fig. 4G and Fig. 2D revealed the difference in chromatographic elution mode, as well as the reliability of this liquid chromatography method for in vitro study. Four major metabolites with the same retention times as those present in drug-containing rat bile (Fig. 4G) could be detected in the RHC system just after 2-minute incubation (Fig. 4D). With a very limited amount of SAA left, no significant increase in the amount of these metabolites was observed after 20-minute incubation (Fig. 4E), indicating metabolism of SAA in this RHC system was completed within 20 minutes. As shown in Fig. 4F, the addition of entacapone would significantly inhibit biotransformation of SAA and accordingly the generation of these metabolites. These results thus confirmed the hepatic contribution to disposition of SAA in rats, as well as the fact that COMT is the enzyme responsible for methylation of SAA.

Structure Elucidation of Methylated Metabolites of SAA. Using Phenomenex Strata-X and repeated ODS column chromatography, four metabolites named M1 through M4 were separated from the in vitro RHC incubation system and their purities were all determined as more than 90% by HPLC analyses (Fig. 5). By using comprehensive

TABLE 1

LC-MS data of drug-containing rat bile (I) and the bile sample hydrolyzed by β-glucuronidase (II)

Retention Time	XIC[a]		[M-H]$^-$ in XIC	Identification
	I	II		
min	*Intensity (% Base Peak)*		*m/z*	
16.56–16.61	4.76×10^5 (100)	1.03×10^6 (100)	493	SAA
34.54–34.58	7.23×10^5 (100)	7.39×10^5 (100)	507	Monomethyl SAA
29.69–29.76	4.34×10^5 (60)	1.99×10^5 (27)		
30.74–30.76	3.61×10^4 (5)	1.85×10^5 (25)		
41.57–41.55	4.66×10^5 (100)	1.74×10^6 (100)	521	Dimethyl SAA
44.33–44.31	3.73×10^5 (80)	5.22×10^5 (30)		
44.87–44.91	3.35×10^5 (72)	1.09×10^6 (63)		
38.51–38.60	1.72×10^5 (37)	3.31×10^5 (19)		
47.89–47.95	1.11×10^5 (24)	6.96×10^4 (4)		
62.80–62.84	2.98×10^5 (100)	3.65×10^5 (100)	535	Trimethyl SAA
52.19–52.22	4.47×10^4 (15)	4.02×10^4 (11)		
10.50–10.52	1.37×10^6 (100)		669	SAA glucuronide
18.25–18.28	1.14×10^6 (100)		683	Monomethyl SAA glucuronide
13.61–13.66	7.07×10^5 (62)			
12.24–12.26	4.67×10^5 (41)			
17.26–17.28	2.51×10^5 (22)			
20.54–20.56	1.71×10^5 (15)			
25.16–25.18	2.84×10^6 (100)		697	Dimethyl SAA glucuronide
31.23–31.26	1.51×10^6 (53)			
16.40–16.42	4.97×10^5 (27)			
10.86–10.88	3.86×10^5 (21)			
19.34–19.36	3.68×10^5 (20)			
34.64–34.66	3.95×10^5 (100)		711	Trimethyl SAA glucuronide
29.36–29.39	2.37×10^5 (60)			
21.92–21.94	1.58×10^5 (40)			

[a]Only those peaks with intensity larger than 3.5×10^4 are listed.

spectroscopic analysis and comparing the spectral data with those of SAA (Sun et al., 2009), the chemical structures of these metabolites were unambiguously elucidated. The spectral data of metabolites M1–M4 are as follows.

M1: A slight yellow powder, $[\alpha]_D^{20}$ +41.5° (*c* 0.1, EtOH). UV (MeOH) λ_{max} (log ε): 288 (4.44), 305 nm (4.39). IR (KBr) ν_{max}: 3385, 1689, 1601, 1519, 1283, 1167, 969, 807 cm^{-1}. ESI-MS *m/z*: 507 [M-H]$^-$, 1037 [2M+Na−2H]$^-$. ^{1}H-NMR (in methanol-*d*4, 400 MHz) δ:7.16 (1H, d, *J* = 1.0 Hz, H-2), 6.79 (1H, d, *J* = 8.2 Hz, H-5), 7.00 (1H, d, *J* = 8.2 Hz, H-6), 7.19 (1H, d, *J* = 16.4 Hz, H-7), 6.65 (1H, d, *J* = 16.4 Hz, H-8), 6.75 (1H, d, *J* = 8.4 Hz, H-5′), 7.12 (1H, d, *J* = 8.4 Hz, H-6′), 8.06 (1H, d, *J* = 15.8 Hz, H-7′), 6.30 (1H, d, *J* = 15.8 Hz, H-8′), 6.72 (1H, d, *J* = 2.0 Hz,H-2″), 6.61 (1H, d, *J* = 8.0 Hz, H-5″), 6.55 (1H, d, *J* = 8.0 Hz, H-6″), 3.06 (1H, d, *J* = 11.4 Hz, H-7″a), 2.93 (1H, d, *J* = 13.8 Hz, H-7″b), 5.12 (1H, d, *J* = 6.9 Hz, H-8″), 3.89 (3H, s, 3-OCH$_3$). ^{13}C-NMR (in methanol-*d*4, 100 MHz) δ: 128.2 (C-1), 120.4 (C-2), 149.2 (C-3), 146.9 (C-4), 110.5 (C-5), 120.6 (C-6), 137.8 (C-7), 116.3 (C-8), 126.3 (C-1′), 131.3 (C-2′), 146.1 (C-3′), 148.2 (C-4′), 116.1 (C-5′), 121.9 (C-6′), 147.8 (C-7′), 116.2 (C-8′), 168.8 (C-9′), 130.0 (C-1″), 117.3 (C-2″), 145.1 (C-3″), 144.4 (C-4″), 114.8 (C-5″), 121.4 (C-6″), 38.3 (C-7″), 74.6 (C-8″), 173.4 (C-9″), 56.4 (C3-OCH$_3$).

M2: A slight yellow powder, $[\alpha]_D^{20}$ +40.2° (*c* 0.1, EtOH). UV (MeOH) λ_{max} (log ε): 287.5 (4.45), 306 nm (4.30). IR (KBr) ν_{max}: 3389, 1686, 1608, 1516, 1276, 1173, 977, 811 cm^{-1}. ESI-MS *m/z*: 507 [M-H]$^-$, 1037 [2M+Na−2H]$^-$. ^{1}H-NMR (in methanol-*d*4, 400 MHz) δ: 7.06 (1H, s, H-2), 6.74 (1H, d, *J* = 8.4 Hz, H-5), 6.90 (1H, d, *J* = 8.2 Hz, H-6), 7.17 (1H, d, *J* = 16.4 Hz, H-7), 6.65 (1H, d, *J* = 16.4 Hz, H-8), 6.97 (1H, d, *J* = 8.4 Hz, H-5′), 7.12 (1H, d, *J* = 8.4 Hz, H-6′), 8.01 (1H, d, *J* = 15.8 Hz, H-7′), 6.30 (1H, d, *J* = 15.8 Hz, H-8′), 6.71 (1H, s, H-2″), 6.63 (1H, d, *J* = 8.0 Hz, H-5″), 6.56 (1H, d, *J* = 8.0 Hz, H-6″), 3.08 (1H, d, *J* = 12.7 Hz, H-7″a), 2.92 (1H, m, H-7″b), 5.11 (1H, br.s, H-8″), 3.86 (3H, s, 3′-OCH$_3$). ^{13}C-NMR (in methanol-*d*4, 100 MHz) δ: 127.9 (C-1), 120.3 (C-2), 146.1 (C-3), 146.4 (C-4), 113.7 (C-5), 120.6 (C-6), 137.3 (C-7), 116.6 (C-8), 126.3 (C-1′), 132.5 (C-2′), 149.2 (C-3′), 148.1 (C-4′), 114.8 (C-5′), 121.9 (C-6′), 147.8 (C-7′), 116.2 (C-8′), 169.0 (C-9′), 130.6 (C-1″), 117.3 (C-2″), 146.0 (C-3″), 144.4 (C-4″), 113.7 (C-5″), 121.0 (C-6″), 38.5 (C-7″), 74.7 (C-8″), 173.4 (C-9″), 56.4 (C3′-OCH$_3$).

M3: A slight yellow powder, $[\alpha]_D^{20}$ +43.8° (*c* 0.05, EtOH). UV (MeOH) λ_{max} (log ε): 287.5 (4.38), 305 nm (4.30). IR (KBr) ν_{max}: 3385, 1688, 1605, 1520, 1282, 1170, 969, 808 cm^{-1}. ESI-MS *m/z*: 521 [M-H]$^-$, 1043 [2M-H]$^-$. ^{1}H-NMR (in methanol-*d*4, 400 MHz) δ: 7.16 (1H, s, H-2), 6.79 (1H, d, *J* = 8.2 Hz, H-5), 7.00 (1H, d, *J* = 8.0 Hz, H-6), 7.20 (1H, d, *J* = 16.4 Hz, H-7), 6.65 (1H, d,*J* = 16.4 Hz, H-8), 6.77 (1H, d, *J* = 7.0 Hz, H-5′), 7.11 (1H, d, *J* = 8.4 Hz, H-6′), 8.08 (1H, d, *J* = 15.8 Hz, H-7′), 6.29 (1H, d, *J* = 15.8 Hz, H-8′), 6.81 (1H, s, H-2″), 6.64 (1H, d, *J* = 8.2 Hz, H-5″), 6.74 (1H, m, H-6″), 3.13 (1H, d, *J* = 11.8 Hz, H-7″a), 2.99 (1H, m, H-7″b), 5.15 (1H, d, *J* = 7.6 Hz, H-8″), 3.89 (3H, s, 3-OCH$_3$), 3.76 (3H, s, 3″-OCH$_3$). ^{13}C-NMR (in methanol-*d*4, 100 MHz) δ: 128.2 (C-1), 120.4 (C-2), 149.2 (C-3), 146.8 (C-4), 110.6 (C-5), 120.6 (C-6), 137.8 (C-7), 116.4 (C-8), 126.2 (C-1′), 131.4 (C-2′), 146.3 (C-3′), 148.2 (C-4′), 116.0 (C-5′), 121.4 (C-6′), 147.8 (C-7′), 116.2 (C-8′), 168.7 (C-9′), 130.9 (C-1″), 114.8 (C-2″), 148.7 (C-3″), 144.4 (C-4″), 114.0 (C-5″), 123.0 (C-6″), 38.6 (C-7″), 74.6 (C-8″), 173.3 (C-9″), 56.5(C3-OCH$_3$), 56.3 (C3″-OCH$_3$).

M4: A slight yellow powder, $[\alpha]_D^{20}$ +42.6° (*c* 0.02, EtOH). UV (MeOH) λ_{max} (log ε): 288 (4.42), 307 nm (4.29). IR (KBr) ν_{max}: 3386, 1690, 1600, 1521, 1277, 1173, 975, 810 cm^{-1}. ESI-MS *m/z*: 521 [M-H]$^-$, 1043 [2M-H]$^-$. ^{1}H-NMR (in methanol-*d*4, 400 MHz) δ: 7.08 (1H, s, H-2), 6.74 (1H, d, *J* =

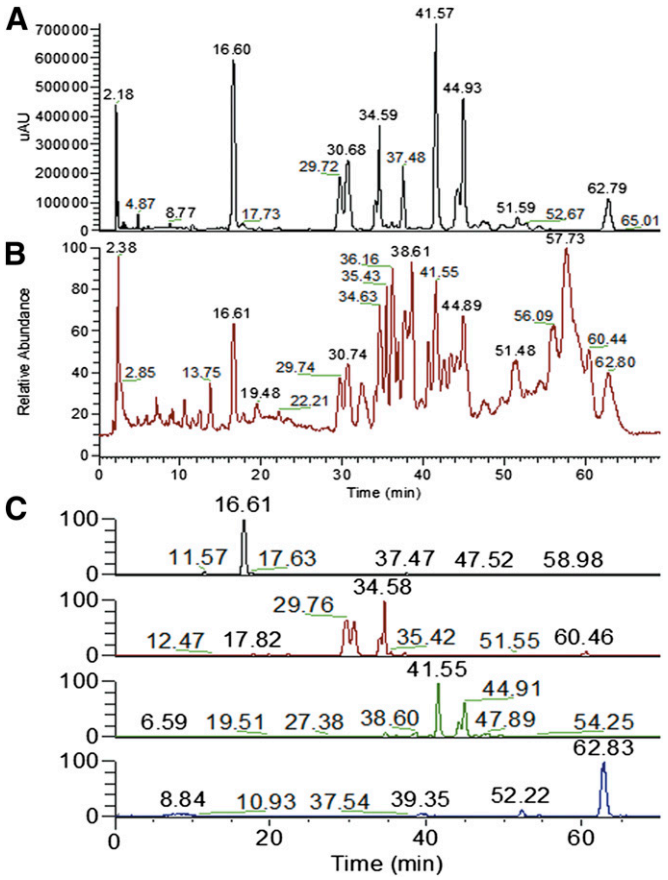

Fig. 3. HPLC-UV (A), TIC (B), and XIC (C) chromatograms of the drug-containing rat bile hydrolyzed by β-glucuronidase. The extracted *m/z* values in the XIC chromatograms were 493, 507, 521, and 535 from top to bottom.

8.4 Hz, H-5), 6.91 (1H, d, J = 8.2 Hz, H-6), 7.18 (1H, d, J = 16.4 Hz, H-7), 6.70 (1H, d, J = 16.4 Hz, H-8), 6.97 (1H, d, J = 8.6 Hz, H-5′), 7.10 (1H, d, J = 8.4 Hz, H-6′), 8.04 (1H, d, J = 15.8 Hz, H-7′), 6.29 (1H, d, J = 15.8 Hz, H-8′), 6.82 (1H, s, H-2″), 6.64 (1H, d, J = 8.0 Hz, H-5″), 6.75 (1H, d, J = 8.0 Hz, H-6″), 3.14 (1H, d, J = 12.9 Hz, H-7″a), 2.99 (1H, m, H-7″b), 5.14 (1H, d, J = 5.8 Hz, H-8″), 3.86 (3H, s, 3′-OCH_3), 3.76 (3H, s, 3″-OCH_3). ^{13}C-NMR (in methanol-d4, 100 MHz) δ: 127.9 (C-1), 120.2 (C-2), 146.2 (C-3), 146.5 (C-4), 113.7 (C-5), 120.6 (C-6), 137.3 (C-7), 116.6 (C-8), 126.3 (C-1′), 132.6 (C-2′), 149.2 (C-3′), 148.2 (C-4′), 114.9 (C-5′), 121.0 (C-6′), 147.8 (C-7′), 116.0 (C-8′), 168.8 (C-9′), 130.4 (C-1″), 112.8 (C-2″), 148.7 (C-3″), 144.5 (C-4″), 113.9 (C-5″), 123.0 (C-6″), 38.7 (C-7″), 74.7 (C-8″), 173.4 (C-9″), 56.4 (C3′-OCH_3), 56.3 (C3″-OCH_3).

The UV and IR spectra of the four metabolites were similar to those of SAA, suggesting that they possessed the same skeleton. The ESI-MS data showed that M1 and M2 had the same molecular ion peaks ($[M-H]^-$) at *m/z* 507, and M3 and M4 at *m/z* 521, which were 14 and 28 mass units higher than SAA, and suggested that they were the isomer pair of monomethyl ether, and dimethyl ether of SAA, respectively. The ^{1}H NMR spectra confirmingly showed signals of one and two methoxyl groups in these two pairs. Because these compounds had the same structure apart from the differences in methoxyl groups, the methylation position could be further determined by detailed analysis including two-dimensional NMR spectra and by comparing the chemical shifts with those of SAA.

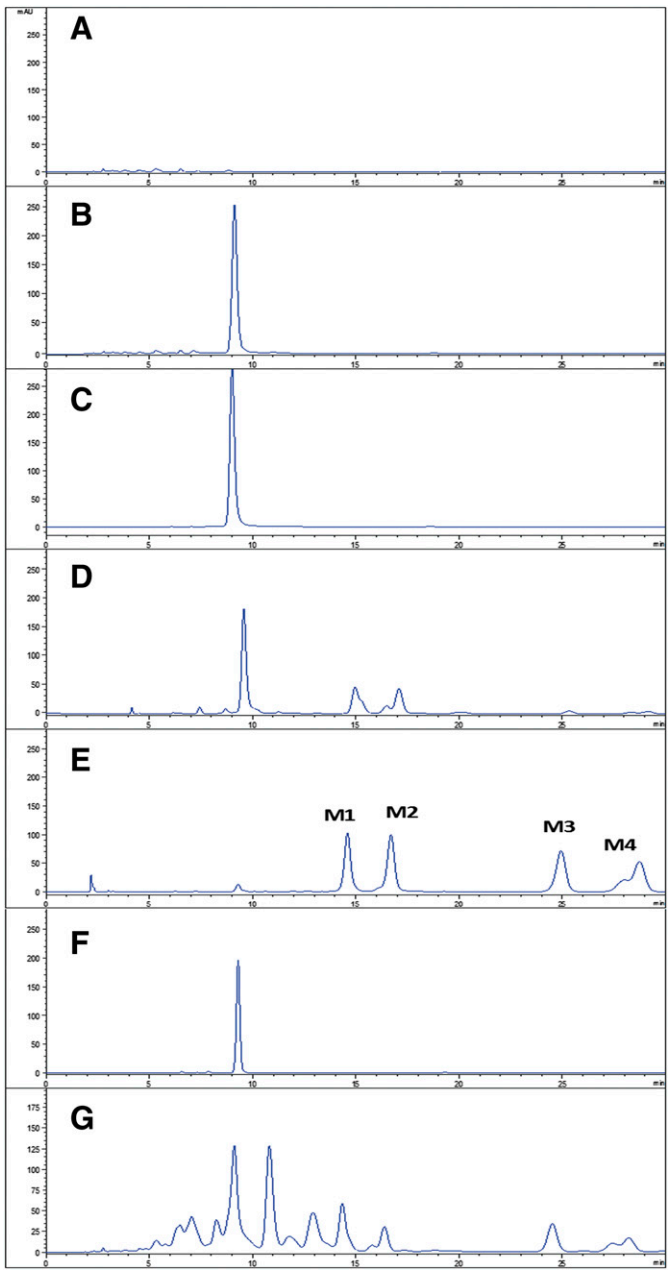

Fig. 4. HPLC chromatograms for incubation study. (A) The reference control of SAA. (B and C) The blank control containing RHC and SAM, and the negative control containing heat-inactivated RHC, SAM, and SAA, respectively, which were both subjected to 20-minute incubation. (D and E) The systems containing RHC, SAM, and SAA for 2-minute and 20-minute incubation, respectively. (F) The system containing RHC, SAM, entacapone, and SAA for 20-minute incubation. (G) The chromatogram of drug-containing rat bile sample obtained under the same HPLC conditions as those of (A) to (E). Peaks M1–M4 indicated the four major metabolites with the same retention time as those present in drug-containing rat bile.

Compared with the SAA parent compound, M1 displayed an additional methoxy carbon signal at δ 56.4 and methoxy proton signal at δ 3.89 (s, 3H). Meanwhile, C-4 was shifted upfield to δ 110.5, and the signals of C-3, H-2, H-6 were shifted downfield to δ 149.2, 7.16, 7.00, respectively. These observed chemical shift changes indicated the substitution effect of methoxy group on electron density of the neighboring groups. Moreover, long-range correlations between the methoxy protons (δ 3.89, 3H) and phenolic carbon at δ 149.2 (C-3) were observed on the ^{1}H-^{13}C heteronuclear multiple-bond correlation spectrum. The chemical structure of M1 was therefore unambiguously determined as

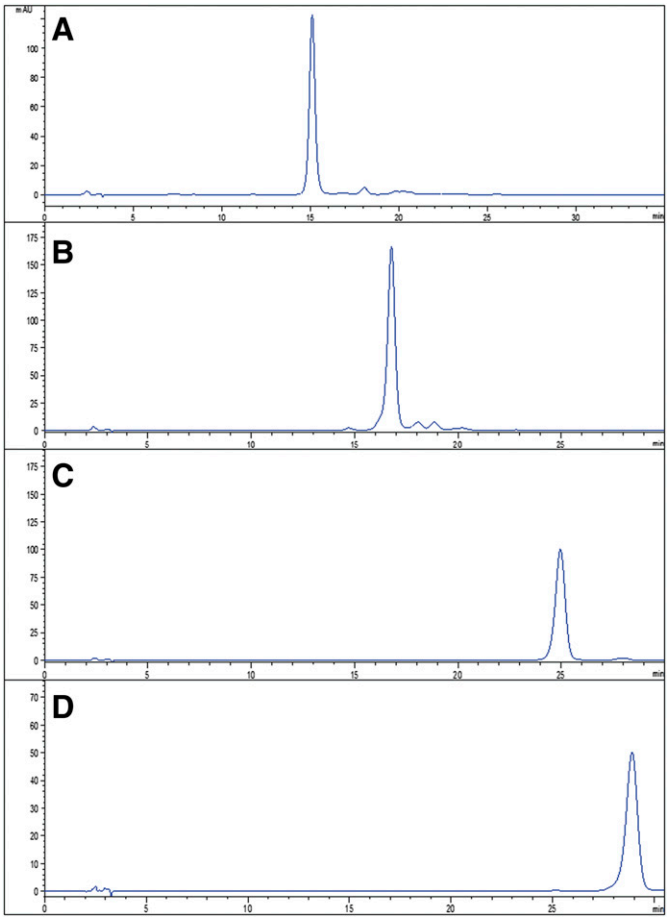

Fig. 5. HPLC chromatograms for purity check of the four methylated metabolites separated from in vitro RHC incubation system. M1, M2, M3, and M4 are shown in (A) through (D), respectively.

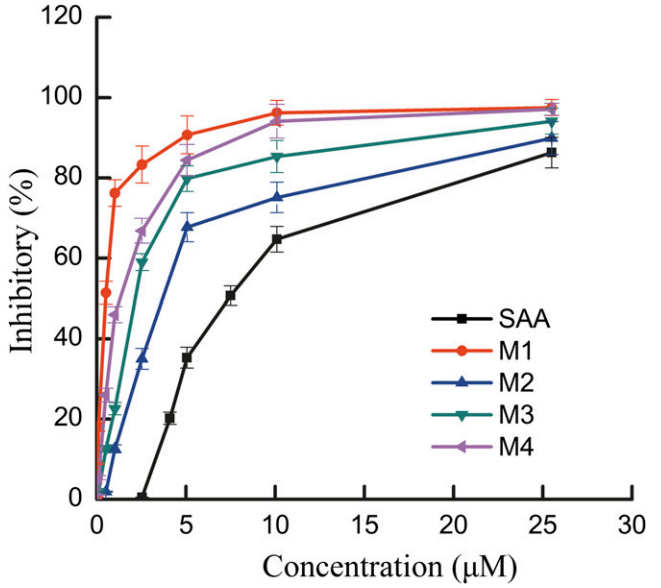

Fig. 6. Inhibitory effects on the formation of TBA reactive substance induced by ferrous ascorbate system in rat liver homogenate in vitro.

3-*O*-methyl-SAA. By the same way, the structures of M2, M3, and M4 were identified as 3′-*O*-methyl-SAA, 3, 3″-*O*-dimethyl-SAA, and 3′, 3″-*O*-dimethyl-SAA, respectively. Such structure characteristics of these metabolites demonstrated that *O*-methylation exclusively resulted in the selective formation of *meta*-*O*-methylated derivatives of SAA. In combination with the findings from the in vitro enzyme inhibition experiment, these results further confirmed that COMT catalyzes the transfer of methyl group from SAM to the *meta*-hydroxyl group of SAA, which is the same for other phenolic compounds with a catechol structure (Axelrod and Tomchick, 1958).

Antioxidant Activities of Methylated Metabolites. It has been proven that antioxidant properties are the basis for various biologic activities of SAA (Lu and Foo, 2002). An investigation of antioxidant potency thus was conducted to evaluate biologic activities of these obtained methylated metabolites of SAA. An in vitro rat liver homogenate lipid peroxidation assay was applied, and BHT (synthetic antioxidant) and α-tocopherol (representative natural antioxidant) were used as positive controls.

As shown in Fig. 6, all of the test compounds displayed a significant inhibitory effect on lipid peroxidation induced by the ferrous ascorbate system and the action was dose dependent within the test concentration ranges. The half-maximal inhibitory concentrations (IC_{50}) on lipid peroxidation reaction were further calculated for quantitative comparison based on dose-response curves. Regarding the positive controls, the IC_{50} values were determined as 146.5 μM and 64.7 μM for α-tocopherol and BHT, respectively. These data were almost the same as those reported by Wang et al. (2000) and Fagali and Catalá (2012); and therefore indicated the reliability of the test results from the present study. SAA and its four methylated metabolites displayed IC_{50} values of 7.48, 0.58, 3.74, 2.77, and 1.65 μM for SAA, and M1–M4, respectively, indicating much stronger antioxidant activities than α-tocopherol and BHT ($P < 0.05$). Moreover, the inhibitory effects on lipid peroxidation significantly increased with methylation of *meta*-hydroxyl groups on the skeleton, and both the methyl-conjugated position and the number of methylation had a certain influence on antioxidant activity of methylated metabolites of SAA.

Discussion

Metabolism involving phase II conjugative reactions occurs generally in SAs and other natural polyphenol compounds (Lv et al., 2010). It has been shown that SAA is metabolized in rats by methylation and glucuronidation into a series of methyl conjugates and their glucuronides, which were previously found in plasma (Shen et al., 2009). Such unique metabolic fate produces a rather complicated metabolism profile of SAA, and isolating these metabolites from excreta is quite challenging.To thoroughly understand the metabolism mechanism of SAA and the activities of its metabolites thus becomes a new challenge.

In summary, metabolism of SAA both in vivo and in vitro was systematically investigated in the present study. Hydrolysis studies using glucuronidase to cleave all of the glucuronides were performed for the drug-containing rat bile. To display the full set of methylation products, LC-MS analysis was conducted for both the hydrolyzed bile sample and the untreated bile, in which XIC filtered chromatograms were applied to resolve suspected coeluting substances, highlight potential metabolite isomers, and then provide clean chromatograms of the metabolite types of interest. The results demonstrated the presence of various methylated metabolites of SAA and its glucuronide in drug-containing bile of rats intravenously administered SAA, which indicated rapid hepatic metabolism and biliary elimination of SAA predominantly in the form of its methylated conjugates. For the first time, four major methylated metabolites present in vivo were prepared by in vitro enzyme-catalyzed incubation with SAM as the methyl donor and RHC

protein as the COMT donor. Their chemical structures were unambiguously identified by NMR and other spectroscopic methods, and in vitro antioxidant activities against rat liver lipid peroxidation were evaluated. The findings confirmed that all of these metabolites are *meta-O*-methylated and COMT is responsible for methylation of SAA. These methylated metabolites displayed fairly high antioxidant potency that was kept at the level of SAA or even significantly increased, suggesting that in vivo pharmacological effects of SAA may be largely related to these metabolites. To acquire a more complete understanding of the metabolism of SAA and the potential pharmacological relevance of its metabolites, further research will be carried out on those underlying methylated metabolites derived from both methylation and glucuronidation. Issues to be addressed may include conjugation position, bioactivity evaluation, structure–activity relationship analysis, and quantitative mass balance of these metabolites.

Acknowledgments

The authors thank Dr. Wenyan Wang for the kind assistance in MS detection and Dr. Li Shen for NMR analysis.

Authorship Contributions

Participated in research design: Xu, Liu.
Conducted experiments: Xu, Li, Che, Tian, Fan.
Performed data analysis: Xu, Li.
Wrote or contributed to the writing of the manuscript: Xu and, Li.

References

Axelrod J and Tomchick R (1958) Enzymatic *O*-methylation of epinephrine and other catechols. *J Biol Chem* **233**:702–705.
Baba S, Osakabe N, Natsume M, and Terao J (2004) Orally administered rosmarinic acid is present as the conjugated and/or methylated forms in plasma, and is degraded and metabolized to conjugated forms of caffeic acid, ferulic acid and m-coumaric acid. *Life Sci* **75**: 165–178.
Chai YY, Wang F, Li YL, Liu K, and Xu H (2012) Antioxidant activities of stilbenoids from *Rheum emodi* Wall. *Evid Based Complement Alternat Med* **2012**:603678.
Cheng TO (2006) Danshen: a versatile Chinese herbal drug for the treatment of coronary heart disease. *Int J Cardiol* **113**:437–438.
Fagali N and Catalá A (2012) The antioxidant behaviour of melatonin and structural analogues during lipid peroxidation depends not only on their functional groups but also on the assay system. *Biochem Biophys Res Commun* **423**:873–877.
Fan HY, Fu FH, Yang MY, Xu H, Zhang AH, and Liu K (2010) Antiplatelet and antithrombotic activities of salvianolic acid A. *Thromb Res* **126**:e17–e22.
Fan HY, Yang L, Fu FH, Xu H, Meng QG, Zhu HB, Teng LR, Yang MY, Zhang LM, and Zhang ZL, et al. (2012) Cardioprotective effects of salvianolic acid a on myocardial ischemia-reperfusion injury *in vivo* and *in vitro*. *Evid Based Complement Alternat Med* **2012**:508938.
Han DE, Zheng Y, Chen XJ, He J, Zhao D, Yang SY, Zhang CF, and Yang ZL (2012) Identification and characterization of human UDP-glucuronosyltransferases responsible for the *in vitro* glucuronidation of salvianolic acid A. *Drug Metab Pharmacokinet* **27**:579–585.
Ho JH and Hong CY (2011) Salvianolic acids: small compounds with multiple mechanisms for cardiovascular protection. *J Biomed Sci* **18**:30–34.
Hou YY, Peng JM, and Chao RB (2007) Pharmacokinetic study of salvianolic acid A in rat after intravenous administration of Danshen injection. *Biomed Chromatogr* **21**:598–601.
Huang YS and Zhang JT (1992) [Antioxidative effect of three water-soluble components isolated from *Salvia miltiorrhiza in vitro*]. *Yao Xue Xue Bao* **27**:96–100.
Ji XY, Tan BKH, and Zhu YZ (2000) Salvia miltiorrhiza and ischemic diseases. *Acta Pharmacol Sin* **21**:1089–1094.
Lian-Niang L, Rui T, and Wei-Ming C (1984) Salvianolic acid A, a new depside from roots of *Salvia miltiorrhiza*. *Planta Med* **50**:227–228.
Liu GT, Zhang TM, Wang BE, and Wang YW (1992) Protective action of seven natural phenolic compounds against peroxidative damage to biomembranes. *Biochem Pharmacol* **43**:147–152.
Lu YR and Foo LY (2002) Polyphenolics of Salvia—a review. *Phytochemistry* **59**:117–140.
Lv YH, Zhang X, Liang X, Liu XR, Dai WX, Yan SK, and Zhang WD (2010) Characterization of the constituents in rat biological fluids after oral administration of Fufang Danshen tablets by ultra-performance liquid chromatography/quadrupole time-of-flight mass spectrometry. *J Pharm Biomed Anal* **52**:155–159.
Pan HJ, Li DY, Fang F, Chen D, Qi LL, Zhang RQ, Xu TD, and Sun H (2011) Salvianolic acid A demonstrates cardioprotective effects in rat hearts and cardiomyocytes after ischemia/reperfusion injury. *J Cardiovasc Pharmacol* **58**:535–542.
Pei LX, Bao YW, Wang HD, Yang F, Xu B, Wang SB, Yang XY, and Du GH (2008) A sensitive method for determination of salvianolic acid A in rat plasma using liquid chromatography/tandem mass spectrometry. *Biomed Chromatogr* **22**:786–794.
Shen Y, Wang XY, Xu LH, Liu XW, and Chao RB (2009) Characterization of metabolites in rat plasma after intravenous administration of salvianolic acid A by liquid chromatography/time-of-flight mass spectrometry and liquid chromatography/ion trap mass spectrometry. *Rapid Commun Mass Spectrom* **23**:1810–1816.
Sun YS, Zhu HF, Wang JH, Liu ZB, and Bi JJ (2009) Isolation and purification of salvianolic acid A and salvianolic acid B from Salvia miltiorrhiza by high-speed counter-current chromatography and comparison of their antioxidant activity. *J Chromatogr B Analyt Technol Biomed Life Sci* **877**:733–737.
Wang JN, Chen YJ, Hano Y, Nomura T, and Tan RX (2000) Antioxidant activity of polyphenols from seeds of *Vitis amurensis in vitro*. *Acta Pharmacol Sin* **21**:633–636.
Wang SB, Tian S, Yang F, Yang HG, Yang XY, and Du GH (2009) Cardioprotective effect of salvianolic acid A on isoproterenol-induced myocardial infarction in rats. *Eur J Pharmacol* **615**:125–132.
Wang XH, Morris-Natschke SL, and Lee KH (2007) New developments in the chemistry and biology of the bioactive constituents of Tanshen. *Med Res Rev* **27**:133–148.
Wang XJ, Wang ZB, and Xu JX (2005) Effect of salvianic acid A on lipid peroxidation and membrane permeability in mitochondria. *J Ethnopharmacol* **97**:441–445.
Wasser S, Ho JM, Ang HK, and Tan CE (1998) Salvia miltiorrhiza reduces experimentally-induced hepatic fibrosis in rats. *J Hepatol* **29**:760–771.
Xu M, Guo H, Han J, Sun SF, Liu AH, Wang BR, Ma XC, Liu P, Qiao X, and Zhang ZC, et al. (2007) Structural characterization of metabolites of salvianolic acid B from *Salvia miltiorrhiza* in normal and antibiotic-treated rats by liquid chromatography-mass spectrometry. *J Chromatogr B Analyt Technol Biomed Life Sci* **858**:184–198.
Zhang Y, Akao T, Nakamura N, Hattori M, Yang XW, Duan CL, and Liu JX (2004) Magnesium lithospermate B is excreted rapidly into rat bile mostly as methylated metabolites, which are potent antioxidants. *Drug Metab Dispos* **32**:752–757.
Zhou LM, Zuo Z, and Chow MSS (2005) Danshen: an overview of its chemistry, pharmacology, pharmacokinetics, and clinical use. *J Clin Pharmacol* **45**:1345–1359.

Address correspondence to: Dr. Ke Liu, School of Pharmacy, Yantai University, Yantai 264005, China. E-mail: ytu309@163.com